Yuan et al. *Zool. Res.* 2022, 43(4): 634−647
https://doi.org/10.24272/j.issn.2095-8137.2022.086

ZR | Zoological Research

Article Open Access

Single-cell transcriptomic landscape of the sheep rumen provides insights into physiological programming development and adaptation of digestive strategies

Yuan Yuan[1,#], Da-Ming Sun[2,3,#], Tao Qin[1,#], Sheng-Yong Mao[2,3], Wei-Yun Zhu[2,3], Yu-Yang Yin[4], Jie Huang[4], Rasmus Heller[5], Zhi-Peng Li[6,*], Jun-Hua Liu[2,3,*], Qiang Qiu[1,*]

[1] *School of Ecology and Environment*, *Northwestern Polytechnical University*, *Xi'an*, *Shaanxi* 710072, *China*

[2] *Ruminant Nutrition and Feed Engineering Technology Research Center*, *College of Animal Science and Technology*, *Nanjing Agricultural University*, *Nanjing*, *Jiangsu* 210095, *China*

[3] *Laboratory of Gastrointestinal Microbiology*, *Jiangsu Key Laboratory of Gastrointestinal Nutrition and Animal Health*, *National Center for International Research on Animal Gut Nutrition*, *College of Animal Science and Technology*, *Nanjing Agricultural University*, *Nanjing*, *Jiangsu* 210095, *China*

[4] *Huzhou Academy of Agricultural Sciences*, *Huzhou*, *Zhejiang* 313000, *China*

[5] *Section for Computational and RNA Biology*, *Department of Biology*, *University of Copenhagen*, *Copenhagen DK*-2200, *Denmark*

[6] *College of Animal Science and Technology*, *Jilin Agricultural University*, *Changchun*, *Jilin* 130118, *China*

ABSTRACT

As an important evolutionary innovation and unique organ, the rumen has played a crucial role in ruminant adaptation to complex ecological environments. However, the cellular basis of its complex morphology and function remains largely unknown. In this study, we identified eight major cell types from seven representative prenatal and postnatal rumen samples using ~56 600 single-cell transcriptomes. We captured the dynamic changes and high heterogeneity in cellular and molecular profiles before, during, and after the appearance of keratinized stratified squamous epithelium with neatly arranged papillae and functional maturity. Basal cells, keratinocytes, differentiating keratinocytes, terminally differentiated keratinocytes, and special spinous cells provided the cellular basis for rumen epithelium formation. Notably, we obtained clear evidence of two keratinization processes involved in early papillogenesis and papillae keratinization and identified *TBX3* as a potential marker gene. Importantly, enriched stratum spinosum cells played crucial roles in volatile fatty

This is an open-access article distributed under the terms of the Creative Commons Attribution Non-Commercial License (http://creativecommons.org/licenses/by-nc/4.0/), which permits unrestricted non-commercial use, distribution, and reproduction in any medium, provided the original work is properly cited.

Copyright ©2022 Editorial Office of Zoological Research, Kunming Institute of Zoology, Chinese Academy of Sciences

Received: 27 May 2022; Accepted: 27 June 2022; Online: 04 July 2022

Foundation items: This work was supported by the Strategic Priority Research Program of the Chinese Academy of Sciences (XDA26040301-02), National Natural Science Foundation of China (31970392, 32172752, 32122083), Research Funds for Interdisciplinary Subject of NWPU (19SH030408), Funds Awarded by the 1000 Talent Project of Shaanxi Province, Project for Top Young Talents Program of College of Animal Science and Technology of Nanjing Agricultural University (DKQB201904), and Talents Team Construction Fund of Jilin Agricultural University.

[#]Authors contributed equally to this work

*Corresponding authors, E-mail: zhplicaas@163.com; liujunhua@njau.edu.cn; qiuqiang@lzu.edu.cn

acid (VFA) metabolism and immune response. Our results provide a comprehensive transcriptional landscape of rumen development at single-cell resolution, as well as valuable insight into the interactions between dietary metabolism and the rumen.

Keywords: Rumen; scRNA-seq; Ruminal epithelium; Keratinization

INTRODUCTION

Ruminants are among the most successful mammalian lineages in animal evolutionary history (Chen et al., 2019). They possess remarkable and distinct multi-chambered stomachs, comprised of the rumen, reticulum, omasum, and abomasum, which collectively form a highly sophisticated natural bioreactor (Lei et al., 2018). This arrangement allows ruminants to utilize plant fiber more efficiently than other mammals, which may have led to their increasing success as extensive swathes of forest were gradually replaced by grassland around 40–50 million years ago (Chen et al., 2019). Consumed plant material is degraded by the dense and diverse microbiota in the rumen into precursors of essential metabolites and metabolic cofactors (particularly volatile fatty acids (VFAs), microbial proteins, and vitamins) used for the production of high-value meat and milk (Xu et al., 2021). Thus, the rumen and associated microbiota play key roles not only in ruminant growth, survival, and reproduction, but also in the provision of highly nutritious food for many human societies (Mizrahi & Jami, 2018). In this symbiotic system, rumen tissue has evolved a series of distinct anatomical features and innovative functions that enable adaptation to the vast, complex rumen microbial ecosystem (Fonty et al., 1991; Russell & Rychlik, 2001). Therefore, elucidating the cellular biological mechanisms underlying rumen formation and development is crucial for understanding the origin and evolution of the organ.

Unlike the stomachs of humans and monogastric animals (with simple, glandular, and prismatic epithelium), rumen tissue has a complex structure consisting of stratified squamous epithelium, lamina propria, mucosa, tunica muscularis, and plasma membrane (Groenewald, 1993; Steven et al., 1970). In contrast to the smooth, non-keratinized stratified squamous epithelium of the esophagus (Oshima et al., 2011), the stratified squamous epithelium of the rumen, including the stratum corneum, granulosum, spinosum, and basal layer, is keratinized like skin epidermis (Graham & Simmons, 2005). This notable structural feature of the rumen not only plays a protective role in defense against microbial invasion but also facilitates renewal of rumen tissue (Graham & Simmons, 2005). This suggests that immunoregulation in the rumen may be involved in maintaining homeostasis, although the idea of the rumen as an immune-related organ remains controversial. Previous transcriptomic analyses have suggested that the *KRT4* gene and keratinocyte differentiation pathway play key roles in stratum corneum formation (Bragulla & Homberger, 2009; Pan et al., 2020). The stratified squamous epithelium is the main site of VFA metabolism and ketogenesis in adult ruminants, thereby affecting the availability of energy and nutrients for the host (Rémond et al., 1995). Immunohistochemical and morphometric analyses have indicated that Na^+-K^+-ATPase α-subunit expression and mitochondrial density and distribution in the stratum spinosum and basal layer of the rumen epithelium facilitate VFA metabolism (Giesecke et al., 1979; Graham & Simmons, 2005). In addition, the rumen contains diverse and interdependent populations of bacteria, archaea, protozoa, fungi, and viruses (Russell & Rychlik, 2001). However, the cellular basis of its complex morphological structure and innovative functions remains largely unknown.

Studying the development of an organ is an effective way to understand its cellular biological foundation (Finnegan et al., 2019; Haber et al., 2017). Morphometric analysis has shown that embryonic sheep rumen tissue forms three differentiated layers at ~42 days of gestation, with the papillary structure and keratinized stratified squamous epithelium forming at ~57 days of gestation (Franco et al., 2011). Postnatal rumen development differs from that of the stomach in monogastric animals. In neonatal ruminants, the fluid (milk or milk replacer) obtained from suckling primarily flows into the abomasum via the esophageal groove in the rumen, resulting in a lack of rumen microbial fermentation substrates to stimulate rumen development (Beharka et al., 1998; Wise & Anderson, 1939). After the introduction of solid food, rumen papillae continue to grow and the VFA metabolism machinery gradually matures (Baldwin & Connor, 2017; Pazoki et al., 2017; Rémond et al., 1995). These findings suggest that dramatic structural and functional changes occur during embryonic and postnatal rumen development, implying that cell type and composition have significantly changed. However, the critical cellular processes that occur during these developmental periods remain unclear.

Here, we performed single-cell RNA sequencing (scRNA-seq) to explore the cellular heterogeneity and function of specific cell types in rumen development. We profiled ~56 600 single-cell transcriptomes from seven key points in sheep rumen development (spanning prenatal to postnatal stages) to address the following questions. First, which cells form the complex morphological structure of the rumen? Second, what processes are involved in the formation of each cell type? Third, which cells play fundamental roles in specific functions and features (keratinization, papilla formation, VFA metabolism, and immunological functions) of the rumen? Our findings should help elucidate the composition, development, and functional maintenance of the rumen at the cellular level and provide valuable insight into the interactions between dietary metabolism and rumen function.

MATERIALS AND METHODS

Sheep rumen dissection

The experimental design and procedures were approved by the Animal Care and Use Committee of Nanjing Agricultural University. Domesticated Hu sheep (a native breed in China with high reproductive efficiency and the ability to tolerate large amounts of roughage) were selected. Prenatal rumen samples were collected from healthy pregnant Hu sheep (at

30, 60, 90, 110, and 130 days of gestation) via caesarean section, and postnatal rumen samples were obtained from newborn and 45-day-old lambs. Fetuses and lambs were stunned by electric shock and killed by exsanguination. The whole rumen was immediately excised and placed in ice-cold phosphate-buffered saline (PBS) (Sigma-Aldrich, USA), after which fatty tissue and blood vessels on the outer wall were carefully removed.

Primary cell isolation

Each rumen sample was incised along the dorsal curvature and washed in cold Hanks' Balanced Salt Solution (HBSS, Gibco, USA) several times to remove mucus and blood. After collecting samples for morphological observation, the rumen tissue was cut into small pieces (5 mm), washed with HBSS until clear, and repeatedly digested with 0.25% trypsin (Gibco, USA) for 25 min at 37 °C. The digestion solution was changed every 5 min, collected in a centrifuge tube containing fetal calf serum, and filtered through a cell strainer (40 μm, Gibco, USA). After solution centrifugation (3 min at 1 500 r/min, 4 °C), the sediment was resuspended in PBS to remove residual trypsin. The fetal rumen cells were centrifuged (3 min at 1 500 r/min, 4 °C) again and resuspended in PBS to determine density and viability using a Bio-Rad TC20 Automated Cell Counter (Bio-Rad, USA). Cell viability was confirmed by trypan blue staining, and cell density was adjusted to 1 000 000 cells/mL. Finally, live cells were selected for scRNA-seq using the 10x Genomics single-cell platform.

ScRNA-seq data processing

Single-cell raw data were processed using 10x Cell Ranger software (v3.0), including "cellranger mkfastq" to demultiplex raw data into Fastq files and "cellranger count" for alignment, filtering, barcode counting, and unique molecular identifier (UMI) counting using default settings. A sheep reference genome (Oar_rambouillet_v1.0) was downloaded from ENSEMBL and built with "cellranger mkgtf". Finally, we obtained seven UMI count tables (absolute numbers of observed transcripts) for further analysis, i.e., one for each developmental stage.

Analysis and visualization of processed sequencing data

For downstream analyses, we retained cells expressing at least 200 genes but less than 25 mitochondrial genes. To obtain a single-cell expression matrix for the retained cells, we applied the "FindIntegrationAnchors" and "IntegrateData" functions in Seurat (v3.1.4) to merge the data and used the "ScaleData" function to regress out mitochondrial gene expression. We then used the "RunPCA" function in Seurat for principal component analysis (PCA) of the corrected cell expression matrix. The number of significant principal components (PCs) was determined using the permutationPA function in the jackstraw R package (https://cran.r-project.org/web/packages/jackstraw). Analysis identified 45 significant PCs, the scores of which were used for further analysis. We then applied the "FindClusters" function in Seurat for cell clustering analysis. We set the parameter resolution to 1.2 and identified 31 clusters. Uniform Manifold Approximation and Projection (UMAP) and t-distributed Stochastic Neighbor Embedding (t-SNE) plots of the second-level clustering results were obtained with Seurat, as above.

Identification of cell types and differentially expressed genes (DEGs)

Differences in gene expression among cell clusters were analysed using the "FindMarkers" function in Seurat. The marker genes visualized in Figure 1C were identified using the FindAllMarkers Seurat function with default settings. The marker genes were analyzed using David (https://david.ncifcrf.gov) for Gene Ontology (GO) and Kyoto Encyclopedia of Genes and Genomes (KEGG) enrichment analyses.

Single-cell pseudo-time trajectory analysis

Monocle (v2.14.0) was used for ordering single cells in pseudo-time (http://cole-trapnell-lab.github.io/monocle-release/ docs/#constructing-single-cell-trajectories). We constructed single-cell differentiation trajectories using Monocle-identified variable genes as ordering genes. Root state was determined based on Seurat cell identity information. Gene clusters were further divided into four clusters according to their *k*-means. To investigate gene function for each gene cluster, we performed GO and KEGG enrichment analyses using David (https://david.ncifcrf.gov).

Statistical analysis

Statistical analyses were performed using the R package. *P*-values were calculated using two-tailed Student's *t*-tests, with values below 0.05 considered statistically significant.

RESULTS AND DISCUSSION

Identification of diverse cell types in rumen

To investigate the key features of rumen development, we collected seven representative Hu sheep rumen samples from the prenatal stage to functional maturity: i.e., at 30, 60, 90, 110, and 130 days of gestation, newborn (at 144 days of gestation), and 45 days old (Figure 1A). We profiled ~56 600 single-cell transcriptomes from these samples and partitioned the cells into 31 clusters (Figure 1B), each containing 194 to 4 291 cells. Based on the distinct expression patterns and levels of known cell-type marker genes (Figure 1C; Supplementary Table S1), we classified these clusters into eight cell types, including epithelial, fibroblast, smooth muscle, endothelial, proliferating, lymphocyte, macrophage, and T cells (Figure 1D).

Epithelial cells, the most variable cell population during rumen development, including basal cells, keratinocytes, differentiating keratinocytes (DKs), terminally differentiated keratinocytes (TDKs), and special spinous cells (SSCs), rapidly increased in proportion at 60 days of gestation (Figure 1E). Clusters 0, 7, and 9 were classified as basal cells with high expression of marker genes such as *KRT15* and *COL17A1* (Joost et al., 2016) (Figure 1C). Cluster 20 cells were annotated as keratinocytes with high expression of *JUN*, *FOS*, and *ZFP36*, which are predominantly expressed in keratinocytes and participate in differentiation (Mehic et al., 2005; Prenzler et al., 2016) (Figure 1C). Clusters 2, 4, 10, 12, 23, 24, and 25 were classified as DKs with high expression of *FABP5*, *KRTDAP*, *SPINK5*, and *CSTA* (Figure 1C), which play roles in keratinocyte differentiation (Finnegan et al., 2019;

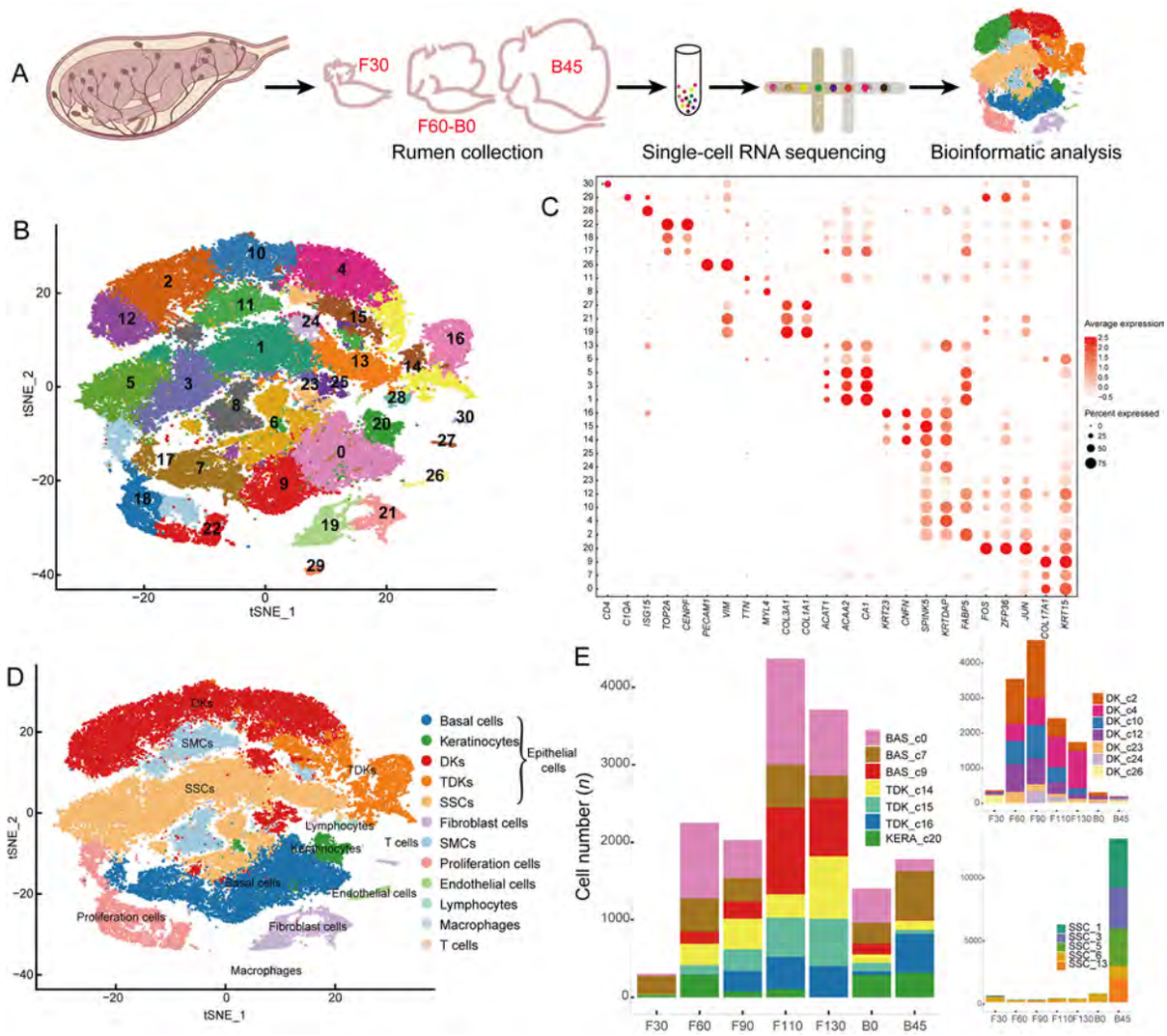

Figure 1 Single-cell transcriptome profiling of sheep rumen

A: Schematic of experimental workflow for scRNA-seq analysis of seven rumen samples. F30, 30 days of gestation; B45, 45 days old. B: t-Distributed stochastic neighbor embedding (t-SNE) plots of rumen cell clusters. The 31 cell clusters are shown in different colors. C: Dot plots of relative gene expression of known cell-type marker genes. Dot size represents percentage of cells expressed, and color intensity represents relative expression level. D: t-SNE plots of identified cell types. Different cell types are shown in different colors. E: Relative proportions of diverse epithelial cell subpopulations at different periods.

Ogawa et al., 2011). Clusters 14, 15, and 16 were classified as TDKs defined by high expression of *CNFN* and *KRT23* (Figure 1C), which are associated with the cornified cell envelope of the stratified squamous epithelium (Wagner et al., 2019). Clusters 1, 3, 5, 6, and 13 were identified as SSCs with high expression of lipid metabolism and ion transport-related genes *CA1*, *ACAA2*, and *BDH1* (Bond et al., 2019) (Figure 1C).

In addition to epithelial cells, Clusters 19, 21, and 27 were identified as fibroblasts with high expression of extracellular matrix (ECM) genes (*COL3A1*, *COL1A1*, *POSTN*, and *DCN*) (Figure 1C) (Han et al., 2020). Clusters 8 and 11 were annotated as smooth muscle cells (SMCs) with high expression of *ACTC1*, *MYL4*, and *TTN* (Han et al., 2020) (Figure 1C). Clusters 17, 18, and 22 were identified as proliferating cells with high expression of cell cycle-related genes, such as *CENPF*, *TOP2A*, and *HIST2H2AC* (Han et al., 2020) (Figure 1C). Cluster 26 cells were annotated as endothelial cells with high expression of *VIM* and *PECAM1* (Han et al., 2020) (Figure 1C). Cluster 28 cells were identified as lymphocytes with high expression of *ISG15*, *MX1*, and *DDX58* (Wani et al., 2019) (Figure 1C), Cluster 29 cells were identified as macrophages due to expression of *C1QA*, *C1QB*, and *C1QC* (Cochain et al., 2018) (Figure 1C), and Cluster 30 cells were identified as T cells expressing *CD4* and *CD69* (Schoenberger, 2012) (Figure 1C).

In summary, scRNA-seq successfully identified cell types of the rumen from the embryonic to functionally mature postnatal stages. This new comprehensive atlas of gene expression and marker genes in diverse cell clusters of the rumen provides a

robust foundation for subsequent studies of rumen development (Table 1).

Diverse cell-type subpopulations in the rumen

Given its importance in diet metabolism and microbial defense, rumen development and functional maturation play crucial roles in ruminant physiology (Baldwin & Connor, 2017). The rumen epithelium develops from two layers of cells at the embryonic state (i.e., stratum basale and stratum granulosum) to a four-layer structure after birth (i.e., stratum basale, stratum spinosum, stratum granulosum, and stratum corneum) (García et al., 2012). Based on the identification of diverse epithelial cell types, we further investigated the genetic characteristics of the four strata of the rumen epithelium. Specific clusters were defined by cell-type abbreviation and cluster number, e.g., BAS-c0 refers to Cluster 0 (basal cells) and DK_c24 refers to Cluster 24 (differentiating keratinocytes).

Basal cells are the main cells in the stratum basale (Jenkins & Tortora, 2016). We identified three basal cell subpopulations (BAS_c0, BAS_c7, and BAS_c9; Figure 2A), which showed high expression of insulin-like growth factor binding protein-related genes (*IGFBP2*, *IGFBP5*, and *IGFBP6*), with particularly strong expression in BAS_c0 and BAS_c9 (Figure 2A; Supplementary Table S2). These genes participate in epithelial-mesenchymal transition (EMT) (Gao et al., 2016; Vijayan et al., 2013), implying that EMT is essential for rumen development at the embryo stage. Furthermore, BAS_c7 cells showed high expression of *HELLS* and *UHRF1* (Figure 2A), which play important roles in epidermal homeostasis (Wang et al., 2020), and of *FABP5*, which participates in keratinocyte differentiation (Ogawa et al., 2011). The proportions of the BAS_c0 and BAS_c9 cells were lower at postnatal day 45 (Figure 1E). We speculate that BAS_c0 and BAS_c9 cells are associated with overall rumen development during the embryonic period and BAS_c7 cells are primarily associated with development of the rumen epithelium.

Keratinocytes are the main cells involved in keratinization (Candi et al., 2005). In addition to keratinocytes (KERA_c20), we identified seven DK subpopulations (DK_c2, DK_c4, DK_c10, DK_c12, DK_c23, DK_c24, and DK_c25) and three TDK subpopulations (TDK_c14, TDK_c15, and TDK_c16) in the rumen (Figure 2B). The relative proportions of DKs and TDKs remained relatively stable throughout the embryonic period (Figure 1E**)**. However, the relative proportions of DK_c2 and DK_c12 decreased, while the relative proportions of DK_c4 and TDK populations increased with development of the embryonic rumen. KEGG pathway enrichment analysis

Table 1 Summary of marker genes of each cell type identified in rumen

Cell type	Marker	Subtype	Marker
Basal cells	*KRT15*, *COL17A1*, *SYNE2*	BAS_c0	*PDLIM4*, *PNISR*, *IGFBP5*
		BAS_c7	*FABP5*, *UHRF1*, *HELLS*
		BAS_c9	*IGFBP6*, *IGF2*, *THEM5*
Keratinocytes	*JUN*, *FOS*, *ZFP36*	–	–
DKs	*FABP5*, *KRTDAP*, *SPINK5*, *CSTA*	DK_c2	*FABP5*, *GSTA1*, *IGFBP2*
		DK_c4	*CSTA*, *IGF2*, *PI3*
		DK_c10	*RBP2*, *MGST1*, *TFF3*
		DK_c12	*IGFBP2*, *IGFBP5*, *IDH1*
		DK_c23	*MT-COX2*, *MT-CYTB*, *MT-ND4*
		DK_c24	*PI3*, *CSTA*, *LYPD1*
		DK_c25	*MT-COX1*, *MT-ND4*, *MT-ATP6*
TDKs	*CNFN*, *KRT23*, *CAST*	TDK_c14	*ANXA1*, *RPS2*, *RPL8*
		TDK_c15	*AHNAK*, *DSP*, *JUP*
		TDK_c16	*S100A9*, *CHMP2A*, *DSTN*
SSCs	*CA1*, *ACAA2*, *BDH1*	SSC_c1	*GSTA1*, *LYPD3*, *KRT17*
		SSC_c3	*TST*, *CA1*, *YBX1*
		SSC_c5	*DHRS7*, *CA12*, *KRT15*
		SSC_c6	*MT-ND3*, *TPM1*, *IGFBP6*
		SSC_c13	*PRD-SPRRII*, *S100A9*, *S100A12*
Fibroblast cells	*COL3A1*, *COL1A1*, *POSTN*, *DCN*	Fibro_c19	*MFAP5*, *DLK1*, *MGP*
		Fibro_c21	*TBX3*, *NDNF*, *APOE*
		Fibro_c27	*GPM6A*, *KRT8*, *LAMP5*
Smooth muscle cells	*ACTC1*, *MYL4*, *TTN*	–	–
Endothelial cells	*VIM*, *PECAM1*, *RAMP2*	–	–
Proliferating cells	*CENPF*, *TOP2A*, *HIST2H2AC*	–	–
Lymphocytes	*ISG15*, *MX1*, *DDX58*	–	–
T cells	*CD4*, *CD69*, *CD53*	–	–
Macrophages	*C1QA*, *C1QB*, *C1QC*	–	–

–: Not available.

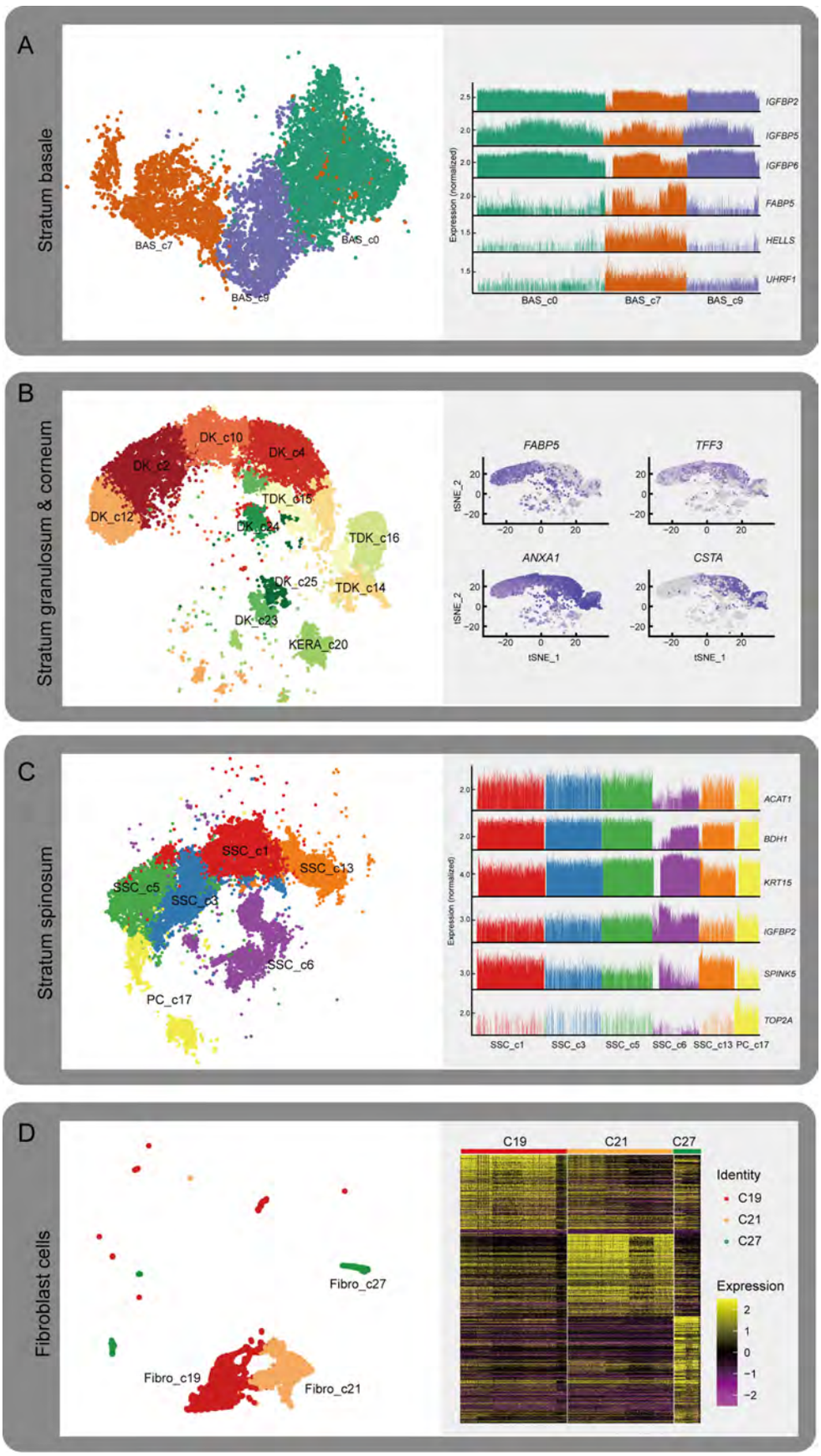
A
Stratum basale
BAS_c7
BAS_c0
BAS_c9
Expression (normalized)
IGFBP2
IGFBP5
IGFBP6
FABP5
HELLS
UHRF1
BAS_c0
BAS_c7
BAS_c9
B
Stratum granulosum & corneum
DK_c10
DK_c4
DK_c2
TDK_c15
DK_c12
DK_c24
TDK_c16
DK_c25
TDK_c14
DK_c23
KERA_c20
FABP5
TFF3
ANXA1
CSTA
tSNE_2
tSNE_1
C
Stratum spinosum
SSC_c1
SSC_c13
SSC_c5
SSC_c3
SSC_c6
PC_c17
Expression (normalized)
ACAT1
BDH1
KRT15
IGFBP2
SPINK5
TOP2A
SSC_c1
SSC_c3
SSC_c5
SSC_c6
SSC_c13
PC_c17
D
Fibroblast cells
Fibro_c27
Fibro_c19
Fibro_c21
C19
C21
C27
Identity
C19
C21
C27
Expression

Figure 2 Characteristics of cell composition and gene expression patterns in the rumen

A: t-SNE plots of three basal cells in stratum basale and relative expression levels of differentially expressed genes (DEGs) in indicated clusters. B: t-SNE plots of cells in stratum granulosum and feature plots showing expression of DEGs in each cluster. C: t-SNE plots of seven cell clusters in stratum spinosum and relative expression of DEGs in each cluster. D: t-SNE plots of three fibroblast subpopulations and heat map of relative expression of DEGs in three fibroblast subpopulations.

indicated that up-regulated DEGs in KERA_c20 cells were enriched in the tumor necrosis factor (TNF) signaling pathway (Supplementary Table S3), which is involved in cell survival, death, and differentiation (Webster & Vucic, 2020), thus suggesting that it may be crucial for keratinocyte differentiation. Comparison of DEGs (Supplementary Table S4) in the DK subpopulations showed that DK_c2 and DK_c10 cells highly expressed *FABP5* and *TFF3* (Figure 2B). *FABP5* induces keratinocyte differentiation through regulation of fatty acid transport (Ogawa et al., 2011), while *TFF3* is a modifying factor in pathways regulating cell proliferation and keratinocyte migration (Storesund et al., 2009). Therefore, these two cell types may be associated with keratinocyte proliferation and differentiation. The DK_c4 and DK_c24 cells highly expressed *ANXA1* and *CSTA* (Figure 2B), which participate in the cornified envelope formation in keratinocytes (Ma & Ozers, 1996; Steven & Steinert, 1994), suggesting that these two subpopulations may be associated with keratinization. The three TDK subpopulations (TDK_c14, TDK_c15, and TDK_c16) showed different gene expression profiles (Figure 3A; Supplementary Table S5). TDK_c14 cells showed high expression of ribosomal protein genes. TDK_c15 cells showed high expression of *AHNAK*, *DSP*, and *JUP*, which are associated with desmoplastic plaques (Masunaga et al., 1995; Yang et al., 2006), indicating a contribution of TDK_c15 to cell adhesion and maintenance of ruminal epithelium stability. TDK_c16 cells showed high expression of innate immune-related genes (*IRF7*, *ISG15*, *FADD*, *MAPK14*, and *MAPK13*), suggesting that the stratum corneum participates in innate immunity in addition to physical defense.

The stratum spinosum is the main metabolic layer of the rumen and can be distinguished morphologically after birth (Baldwin & Connor, 2017). Comparison of the proportions of epithelial cells in different periods showed that five clusters (proliferating cell cluster PC_c17 and SSC clusters SSC_c1, SSC_c3, SSC_c5, and SSC_c13) were significantly more abundant at postnatal day 45 (Figure 1E). These five subpopulations showed high expression of key ketogenesis-related genes (*ACAT1*, *SLC16A1*, and *BDH1*) (Figure 3B; Supplementary Table S6). Ketogenesis is a hallmark of metabolic development of the rumen epithelium (Naeem et al., 2012). Therefore, we defined these five cell clusters as the

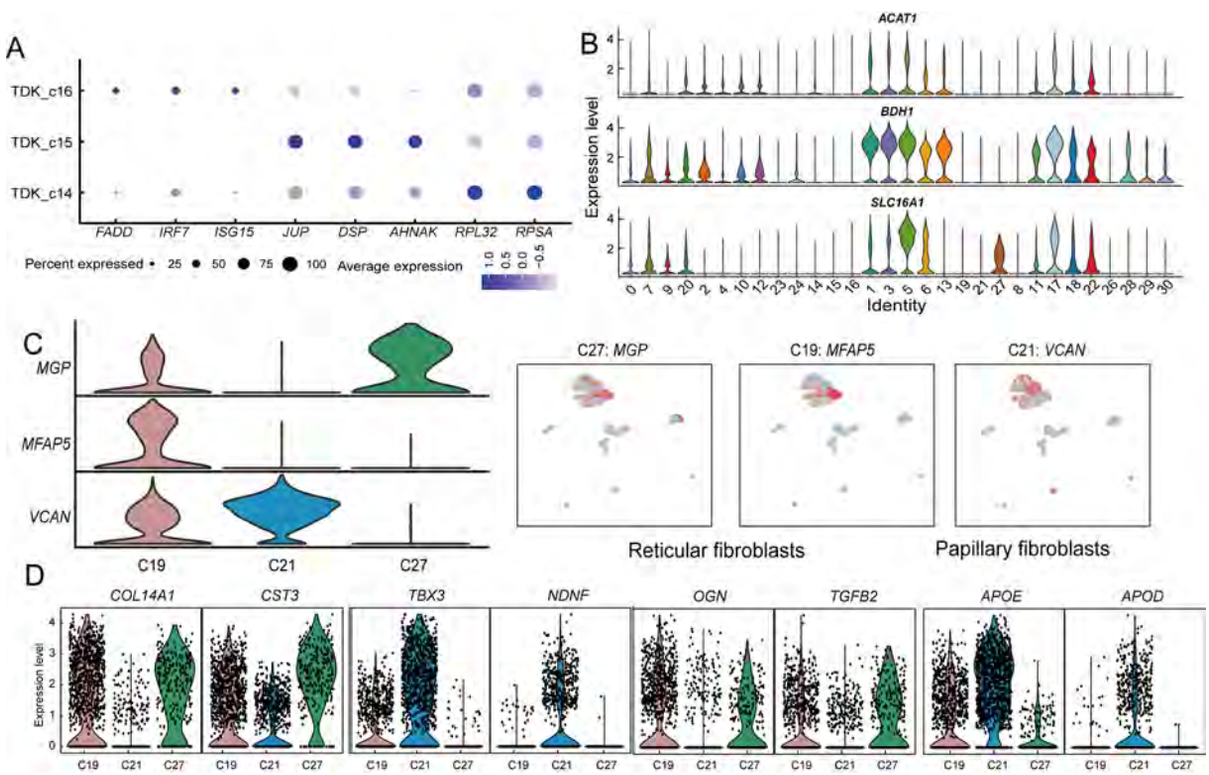

Figure 3 Expression of selected genes across rumen cell populations

A: Dot plot of relative gene expression of DEGs in three TDK subpopulations. Dot size represents percentage of cells expressed, and color intensity represents relative expression level. B: Violin plots showing expression of selected genes in cell clusters. C: Feature plots of three classes of fibroblast marker genes. D: Violin plots of DEGs in three fibroblast types.

major cell types of the rumen epithelium stratum spinosum. Among the SSC subpopulations, SSC_c5 cells exhibited high expression of metabolic genes and marker genes of basal cells (*KRT15* and *IGFBP2*) (Figure 2C), suggesting that they have a similar differentiation capacity to basal cells. SSC_c3 cells showed high expression of mitochondrial genes, suggesting a major role in energy metabolism. SSC_c1 and SSC_c13 cells showed high expression of *SPINK5* and *PRD-SPRRII*, indicating that these two subpopulations exhibited the highest degree of keratinization. Interestingly, PC_c17 cells expressed more ketogenesis-related genes than other proliferating cells (PC_c18 and PC_c22), suggesting that PC_c17 may represent the proliferative state of SSCs (Figures 2C, 3B). Thus, we hypothesize that the SSC and PC_17 cell subpopulations may play key roles in the renewal and proliferation of the stratum spinosum, thereby maintaining the homeostasis of rumen metabolic function.

Fibroblasts, which are enriched in the rumen lamina propria, not only produce extracellular matrix (ECM) to provide structural support for the epithelium, but also participate in cell signaling, migration, proliferation, and differentiation (Kim et al., 2011). We identified three types of fibroblasts (Clusters 19, 21, and 27) in the rumen (Figure 2D). Both C19 and C27 cells showed high expression of *COL14A1* (collagen-encoding gene) and *MGP* in comparison with C21 but could be distinguished by differential expression of *MFAP5* and *KRT8* (Figure 3C). C21 cells strongly expressed lipid transport-related genes *APOE* and *APOD* and collagen-encoding gene *COL13A1* (Figure 3D). Comparison of the DEGs in the three fibroblast types indicated that C21 consisted of papillary fibroblasts, while C19 and C27 consisted of reticular fibroblasts. We further found that the papillary fibroblasts (C21) strongly expressed neuro-development (*NDNF*)-related genes, suggesting that papillary fibroblasts also participate in rumen innervation (Figure 3D).

In summary, combined with the characteristics of the rumen structure, we identified specific cell types associated with the morphological strata of the rumen and the heterogeneity of cells in these strata. Different cell subpopulations showed specific gene expression characteristics and different functions during rumen development.

Characterization of dynamic prenatal and postnatal rumen developmental patterns

Based on morphometric analysis (Figure 4A) and expression characteristics of samples obtained from seven periods of

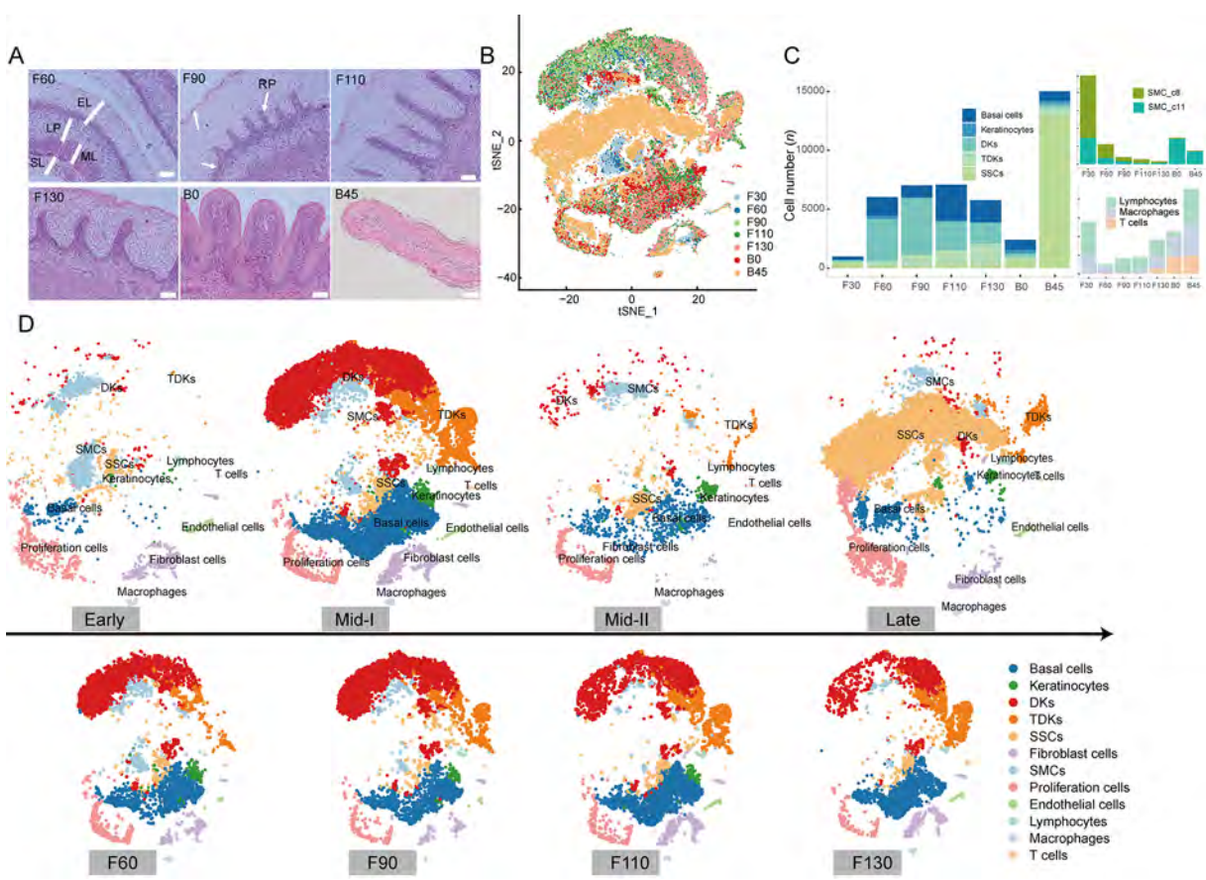

Figure 4 Characterization of rumen developmental patterns

A: Schematic of rumen development, as elucidated in this study, illustrating typical changes in morphology observed during rumen development. EL, epithelial layer; LP, lamina propria; ML, muscularis layer; SL serosa layer; RP, ruminal pillars. B: t-SNE plots of cell clusters, colored according to indicated periods of rumen development. C: Proportions of cells of indicated types at indicated sampling times. D: t-SNE plots of cell clusters at four developmental stages and four periods of middle-I stage.

rumen development (Figure 4B; Supplementary Table S7), we distinguished four major stages of development, i.e., early (0–30 days of gestation), middle-I (60, 90, 110, and 130 days of gestation), middle-II (newborn), and late (45 days old) (Figure 4D).

During the early stage of rumen development, the rumen becomes a small separate compartment of the primitive gastric tube. The ruminal wall consists of four layers: i.e., internal epithelial layer, middle pluripotential blastemic tissue layer, tunica muscularis (with an inner circular layer and outer longitudinal layer), and serosa (García et al., 2012; Jenkins & Tortora, 2016). Cell-type analysis showed that all cell types were present in the early stage, but SMCs were dominant (Figure 4C). We identified two SMC clusters (SMC_c8 and SMC_c11), which corresponded to the inner circular layer and outer longitudinal layer of the tunica muscularis (Martini, 2006). In addition, scRNA-seq confirmed the presence of immune cells (lymphocytes, macrophages, and T cells) in the early-stage rumen (Figure 4C), which has been controversial due to their small numbers and difficult detection by conventional methods.

In the middle-I stage of rumen development, the ruminal wall consisted of four layers: i.e., epithelium, lamina propria + submucosa, tunica muscularis, and serosa (Figure 4A). Morphological changed include ruminal papillogenesis and maturation of the epithelial layer (Figure 4A). With the formation of the rumen epithelium, several epithelial cells (basal cells, keratinocytes, DKs, TDKs) became the dominant type in the rumen, and the proportions of all epithelial cell types increased significantly at 60 days of gestation (Figure 4C). We also observed significant changes in the proportions of various epithelial cell types with increasing gestation time (Figure 1E, 4C). The percentages of keratinocytes and TDKs decreased and increased with gestation time, respectively (Figure 4C), coinciding with gradual keratinization during rumen development (Figure 4A). Furthermore, at 90 days of gestation, we found that early epithelial stratification was accompanied by slight elongation of the stratum germinativum into the stratum granulosum, forming rudimentary ruminal papillae (Figure 4A). Accordingly, the proportion of DK_c24 cells was higher at 90 days than at 60 days of gestation, suggesting that these cells may be associated with early papillogenesis. Hence, the dynamic changes in different epithelial cell types provide the cellular basis for the specific morphology of the mature rumen (keratinization, papilla formation) at this developmental stage.

In the middle-II stage, the rumen papilla structure formed and the epithelium differentiated into four layers: i.e., stratum corneum, stratum granulosum, stratum spinosum, and stratum basale (Figure 4A). We found that the proportions of basal cells, keratinocytes, TDKs, and SSCs in this stage were relatively balanced, while the proportions of DKs and fibroblasts decreased. In addition, the proportion of SSCs, major contributors to the metabolic capacity of the rumen, highly increased (Figure 4C), indicating that newborns formed a metabolically competent rumen before receiving external food stimulation, although SSCs were not the dominant cell type at this stage.

In the late stage of rumen development, SSCs became the dominant cell type, accounting for ~85% of the rumen cell population, and proliferating cells increased significantly (Supplementary Table S8). These findings suggest that dramatic changes in rumen cell composition are adaptive responses to the external environment after solid diet introduction. Overall, these results reveal the dynamic changes in cell type and proportion that occur during rumen development in sheep, providing valuable clues for large-scale studies of rumen development in ruminants.

Characteristics of keratinization and papillogenesis during rumen development

Ruminal parakeratosis is a common ruminant disease caused by abnormal keratinization (Underwood et al., 2015), which impairs ruminant health and production by affecting defense and absorption of the rumen epithelium (Steele et al., 2009). We explored rumen keratinization in the current study. Based on pseudo-time analysis (Guo et al., 2021), we identified two distinct keratinization processes during normal rumen development (Figure 5A). One process (designated P1) involved progression through basal, KERA_c20, DK_c12, DK_c2, DK_c10, DK_c4, and TDK cellular states. The other process (designated P2) involved progression through basal, KERA_c20, DK_c12, DK_c2, DK_c10, DK_c24, DK_c4, and TDK cellular states (Figure 5B). These two keratinization processes exhibited similar dynamic gene expression profiles (Figure 5C, D), although passage through the DK_c24 state was only observed in P2. The DK_c24 cells showed high expression of *PI3* (Supplementary Table S4), which is associated with elongation of the lateral cell membrane (Wang & Brieher, 2020), and a rapid increase in abundance in the early papillogenesis phase at prenatal day 90. We hypothesize that DK_c24 cells are a transitional state for keratinocytes that appear during early papillogenesis of the rumen, and P2 is the process of papillae keratinization.

To further elucidate the P2 keratinization process, we visualized dynamic gene expression patterns along the pseudo-time trajectory and classified them into four groups (Figure 5C; Supplementary Table S9). Group 1 contained 317 genes highly expressed in early keratinization, including *SOX2*, *MEIS1*, *RIF1*, *APC*, *ID3*, *SMARCAD1*, *SMAD5*, and *FGFR2* (Figure 5E), which are associated with regulation of stem cell pluripotency (Kanehisa et al., 2021). These genes were enriched in the GO terms “nucleoplasm” and “DNA binding”, suggesting that cell differentiation is a major step in early keratinization (Supplementary Table S10). The main keratin-encoding gene in this group was *KRT17* (Figure 5E). Group 2 included 364 genes highly expressed in the mid-stage of keratinization, including genes associated with mitochondrial formation, maintenance, and function. These genes were enriched in the “Ribosome” pathway, indicating high rates of protein synthesis (Supplementary Table S10). The main keratin-encoding gene expressed in this group was *KRT15* (Figure 5E). Group 3 contained 306 genes highly expressed in the mid-stage of keratinization, including *KRT4*, *ANXA7*, *VDAC1*, and *CNN3* (Figure 5E), which are associated with epithelial cell differentiation (Kanehisa et al., 2021). These genes were enriched in the GO terms “microtubule” and “focal adhesion” (Supplementary Table S10), suggesting

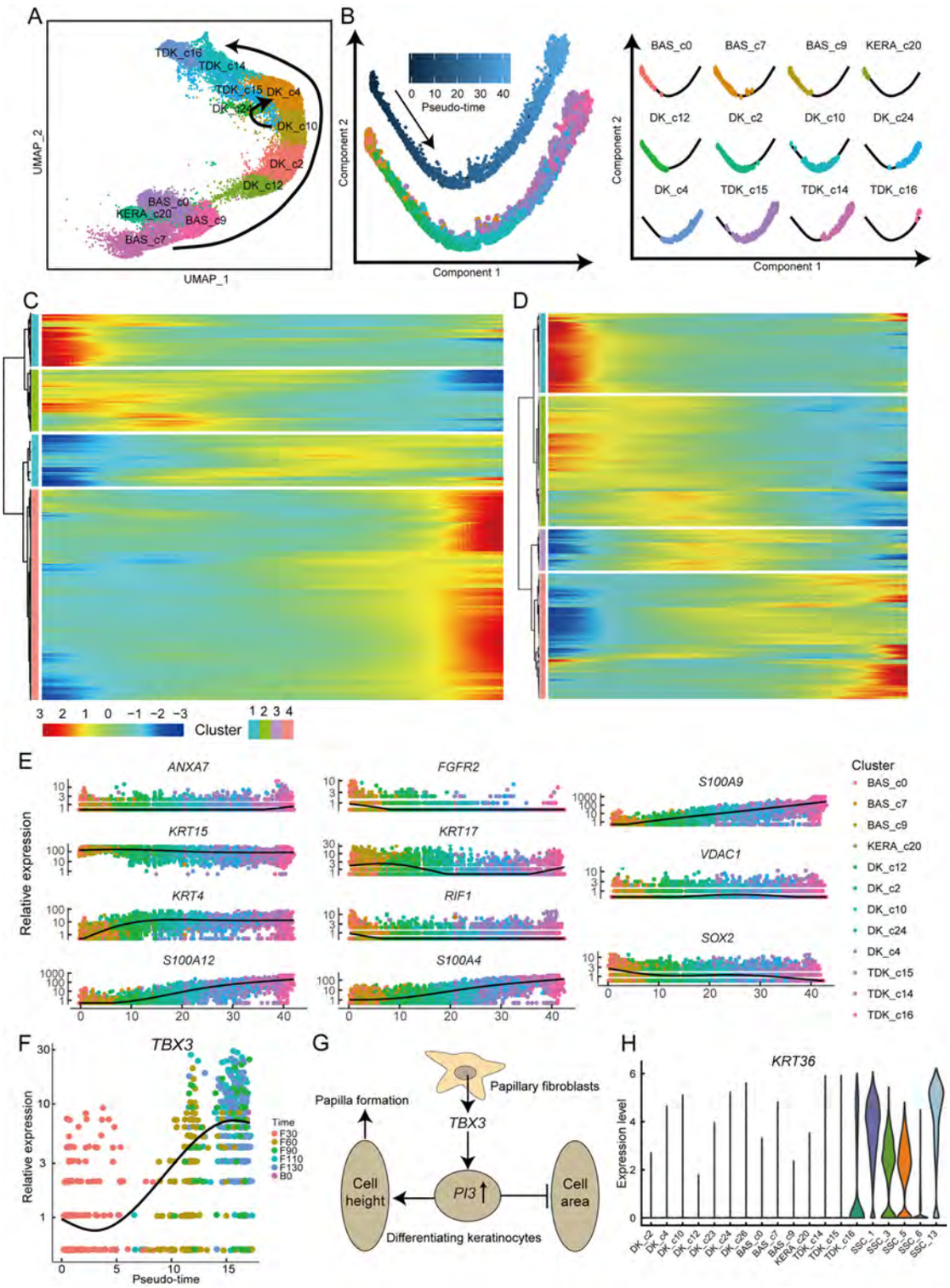

Figure 5 Molecular features of keratinization and papillogenesis during rumen development

A: UMAP plot of epithelial cells showing keratinization process at cellular level. B: Pseudo-time trajectory of P2 keratinization process and deconvolution of pseudo-time plot according to cell type. C: Heatmap showing four clusters of pseudo-time genes differentially expressed with P2 keratinization. D: Heatmap showing four clusters of pseudo-time genes differentially expressed with P1 keratinization. E: Expression levels of representative genes in cells ordered along trajectory (colored based on clusters to which they are assigned). F: Changes in expression patterns of *TBX3* gene in papillary fibroblasts over time. Cells are color-coded with rumen samples. G: Schematic of papillary development. H: Violin plots showing relative expression of *KRT36* in diverse epithelial cell subpopulations.

that cellular connections are enhanced during this stage of keratinization. Group 4 contained 1242 genes highly expressed in late keratinization and enriched in the KEGG terms “adhesion junction” and “bacterial invasion of epithelial cells” (Supplementary Table S10). Genes of the S100A family (*S100A2*, *S100A4*, *S100A5*, *S100A9*, *S100A10*, *S100A12*, and *S100A13*), which are associated with the immune system (Xia et al., 2018), were also highly expressed in the late stage (Figure 5E), indicating that the rumen epithelium develops defensive capacities in this stage.

The neatly arranged papillae are a striking morphological feature of the mature rumen, enlarging the surface area available for nutrient absorption and metabolism (Graham & Simmons, 2005). Anormogenesis of rumen papillae can trigger subacute ruminal acidosis and other nutritional metabolic diseases that can severely impair animal production and health (Underwood et al., 2015). Papillary fibroblasts, which are close to the epithelial layer and associated with papilla formation, showed higher *TBX3* transcription factor expression than the reticular fibroblasts (Figure 5F). Previous studies have shown that abnormal expression of *TBX3* in humans can cause papillary carcinoma of the skin, ulnar-mammary syndrome, and arrhythmia (Frank et al., 2012; Khan et al., 2020). High *TBX3* expression can also promote expression of *PI3* (Peres et al., 2015), which was strongly expressed in the papillogenesis-related DK_c24 cells. We speculate that the increased expression of *TBX3* in the papillary fibroblasts may promote an increase in *PI3* expression in the DK_c24 cells, leading to elongation of the lateral membrane of the epithelial cells and hence papillogenesis (Figure 5G). In addition, we found that the five cell clusters in the stratum spinosum highly expressed *KRT36* (Figure 5H), a specific marker of filiform papillae (Brychtova et al., 2020). This suggests that stratum spinosum cells are in the papillae and corroborates the importance of rumen papillae as sites of energy metabolism.

Functional rumen epithelium formation after birth

With the introduction of a solid diet after birth, the proportion of SSCs (1, 3, 5, and 13) and PC_c17 cells increased and became dominant in the rumen epithelium and formed the stratum spinosum by postnatal day 45. We identified 407 genes highly expressed in SSCs. KEGG enrichment analysis of up-regulated DEGs revealed that 73 genes were enriched in metabolic pathways, including carbon metabolism, fatty acid metabolism, propanoate metabolism, and butanoate metabolism (Supplementary Tables S11, S12). These findings suggest that the major cellular components required for a functionally mature rumen epithelium are established before postnatal day 45.

As ruminants are exposed to a highly complex environment from birth, the rumen must not only develop physical defenses, but also an immune response. However, there were no significant differences in the expression levels of immune-related genes among the three types of immune cells in the rumen before and after birth (Figure 6A). Interestingly, we found that SSC_c13 was the most keratinized subpopulation of SSCs, and cells in this cluster showed high expression of immune-related genes (*ISG15*, *IL36A*, and S100A gene family) (Figure 6B). *ISG15* plays a key role in the innate immune system, inducing natural killer cell proliferation (Perng & Lenschow, 2018). *ISG15* also induces interferon (IFN) cytokines as an anti-mycobacterial response and is highly expressed in lymphocytes (Gao et al., 2020). Thus, we hypothesize that SSC_c15 cells induce lymphocyte proliferation to generate an immune response. These findings suggest that maturation of the postnatal rumen stratum spinosum is not only important for ruminant energy

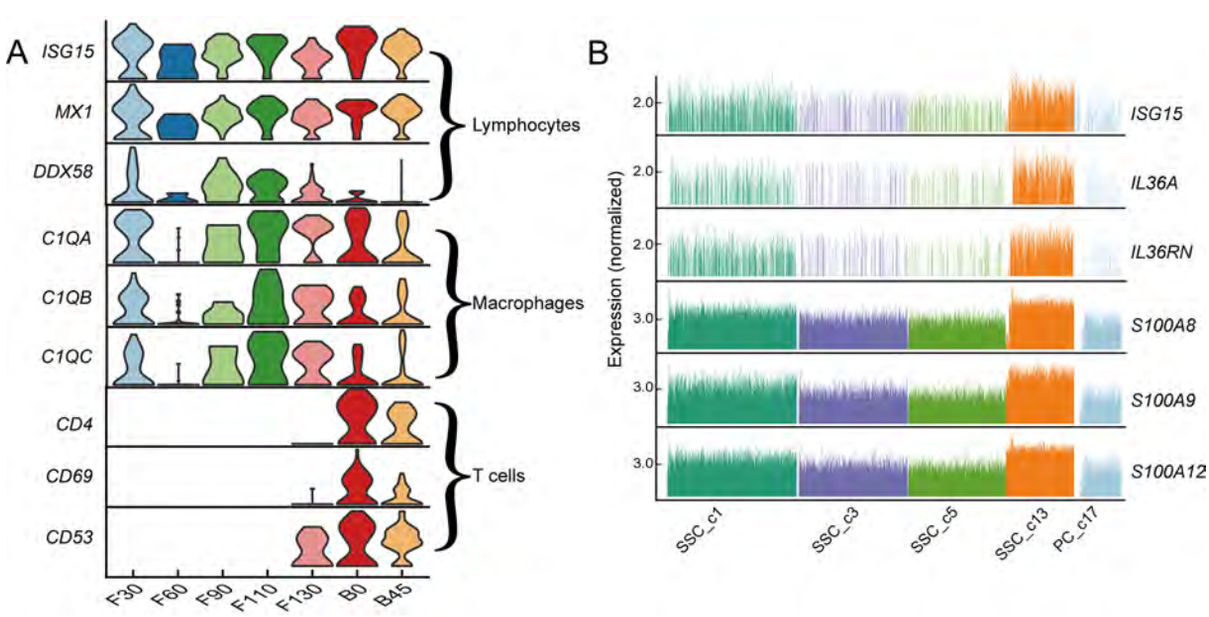

Figure 6 Molecular features of various cell types in rumen of lambs after birth

A: Violin plots showing expression of marker genes of three immune cell types at different developmental stages. B: Relative expression levels of immune-related genes in SSCs.

metabolism, but also for immune capacity.

CONCLUSIONS

As an important evolutionary innovation and unique organ, the rumen has played an important role in the adaptation of ruminants to their complex ecological environments. This study provides a detailed account of gene expression during prenatal to postnatal rumen development based on scRNA-seq analysis, including detailed characterization of the cell types involved, as well as identification of additional marker genes for specific cell types. We revealed the dynamic changes and high heterogeneity of the cellular and molecular profiles during four development stages of the rumen, providing clues for maternal regulation of fetal rumen development. However, this study is limited by the small sample size and number of captured cells.

The rumen has evolved a series of distinct structural hallmarks, such as neatly arranged papillae and keratinized stratified squamous epithelium, as well as innovative functional characteristics, such as VFA metabolism and immunology. Our identification of diverse basal cells, keratinocytes, DKs, TDKs, and SSCs provides important insight into rumen structure and function and a basis for isolating different cells in the rumen. The epithelial cells exhibit two processes during papillary keratinization accompanied by dynamic changes in identified gene expression. In addition, the cellular and gene expression profiles strongly suggested that the rumen epithelium is functionally mature by postnatal day 45, and the enriched stratum spinosum cells play crucial roles in VFA energy metabolism and immune capacity. Importantly, we identified the growth factor *TBX3* as a potential marker gene for papillary growth by interacting with *PI3*, thus highlighting the need to validate the role of *TBX3* in papillogenesis *in vivo* and *in vitro*.

Our findings provide cellular-level insights into the molecular characteristics of morphogenesis, notably keratinization and papilla formation, and functional establishment (metabolism and immunity) of the rumen. This study will contribute to our understanding of rumen development and the interactions between dietary metabolism and the rumen.

DATA AVAILABILITY

The single-cell RNA-sequencing data were deposited in the Genome Sequence Archive database (http://gsa.big.ac.cn/) under accession No. CRA007511, Science Data Bank (doi:10.577 60/sciencedb.j00139.00007), and NCBI under BioProjectID PRJNA857336.

SUPPLEMENTARY DATA

Supplementary data to this article can be found online.

COMPETING INTERESTS

The authors declare that they have no competing interests.

AUTHORS' CONTRIBUTIONS

Q.Q., J.H.L., Z.P.L., and S.Y.M. designed the project and research; D.M.S., J.H.L., W.Y.Z., Y.Y.Y., and J.H. collected samples and constructed sequencing libraries; Y.Y., D.M.S., and T.Q. conducted single-cell data analysis; Q.Q., J.H.L., Z.P.L., and Y.Y. wrote the manuscript. Q.Q., J.H.L., Z.P.L., R.H., and Y.Y. amended the manuscript. All authors read and approved the final version of the manuscript.

REFERENCES

Baldwin RL, Connor EE. 2017. Rumen function and development. *Veterinary Clinics of North America:Food Animal Practice*, **33**(3): 427−439.

Beharka AA, Nagaraja TG, Morrill JL, Kennedy GA, Klemm RD. 1998. Effects of form of the diet on anatomical, microbial, and fermentative development of the rumen of neonatal calves. *Journal of Dairy Science*, **81**(7): 1946−1955.

Bond JJ, Donaldson AJ, Coumans JVF, Austin K, Ebert D, Wheeler D, et al. 2019. Protein profiles of enzymatically isolated rumen epithelium in sheep fed a fibrous diet. *Journal of Animal Science and Biotechnology*, **10**(1): 5.

Bragulla HH, Homberger DG. 2009. Structure and functions of keratin proteins in simple, stratified, keratinized and cornified epithelia. *Journal of Anatomy*, **214**(4): 516−559.

Brychtova V, Coates PJ, Hrabal V, Boldrup L, Fabian P, Vojtesek B, et al. 2020. Keratin 36, a specific marker of tongue filiform papillae, is downregulated in squamous cell carcinoma of the mobile tongue. *Molecular and Clinical Oncology*, **12**(5): 421−428.

Candi E, Schmidt R, Melino G. 2005. The cornified envelope: a model of cell death in the skin. Nature reviews *Molecular Cell Biology*, **6**(4): 328–340.

Chen L, Qiu Q, Jiang Y, Wang K, Lin ZS, Li ZP, et al. 2019. Large-scale ruminant genome sequencing provides insights into their evolution and distinct traits. *Science*, **364**(6446): eaav6202.

Cochain C, Vafadarnejad E, Arampatzi P, Pelisek J, Winkels H, Ley K, et al. 2018. Single-cell RNA-seq reveals the transcriptional landscape and heterogeneity of aortic macrophages in murine atherosclerosis. *Circulation Research*, **122**(12): 1661−1674.

Finnegan A, Cho RJ, Luu A, Harirchian P, Lee J, Cheng JB, et al. 2019. Single-cell transcriptomics reveals spatial and temporal turnover of keratinocyte differentiation regulators. *Frontiers in Genetics*, **10**: 775.

Fonty G, Jouany JP, Chavarot M, Bonnemoy F, Gouet P. 1991. Development of the rumen digestive functions in lambs placed in a sterile isolator a few days after birth. *Reproduction Nutrition Development*, **31**(5): 521−528.

Franco A, Masot J, Redondo E. 2011. Ontogenesis of the rumen: a comparative analysis of the Merino sheep and Iberian red deer. *Animal Science Journal*, **82**(1): 107−116.

Frank DU, Carter KL, Thomas KR, Burr RM, Bakker ML, Coetzee WA, et al. 2012. Lethal arrhythmias in *Tbx3*-deficient mice reveal extreme dosage sensitivity of cardiac conduction system function and homeostasis. *Proceedings of the National Academy of Sciences of the United States of America*, **109**(3): E154−E163.

Gao N, Me R, Dai C, Yu FSX. 2020. ISG15 acts as a mediator of innate immune response to *Pseudomonas aeruginosa* infection in C57BL/6J mouse corneas. *Investigative Ophthalmology & Visual Science*, **61**(5): 26−26.

Gao S, Sun Y, Zhang XB, Hu LM, Liu YX, Chua CY, et al. 2016. IGFBP2 activates the NF-κB pathway to drive epithelial–mesenchymal transition and invasive character in pancreatic ductal adenocarcinoma. *Cancer Research*, **76**(22): 6543−6554.

García A, Masot J, Franco A, Gázquez A, Redondo E. 2012. Histomorphometric and immunohistochemical study of the goat rumen during prenatal development. *The Anatomical Record:Advances in Integrative Anatomy and Evolutionary Biology*, **295**(5): 776−785.

Giesecke D, Beck U, Wiesmayr S, Stangassinger M. 1979. The effect of rumen epithelial development on metabolic activities and ketogenesis by the tissue *in vitro*. *Comparative Biochemistry and Physiology Part B: Comparative Biochemistry*, **62**(4): 459–463.

Graham C, Simmons NL. 2005. Functional organization of the bovine rumen epithelium. *American Journal of Physiology-Regulatory, Integrative and Comparative Physiology*, **288**(1): R173−R181.

Groenewald HB. 1993. Ultrastructure of the epithelium of the rumen, reticulum and omasum of grey, white and black karakul lambs. *Onderstepoort Journal of Veterinary Research*, **60**(3): 197−204.

Guo JT, Sosa E, Chitiashvili T, Nie XC, Rojas EJ, Oliver E, et al. 2021. Single-cell analysis of the developing human testis reveals somatic niche cell specification and fetal germline stem cell establishment. *Cell Stem Cell*, **28**(4): 764−778.e4.

Haber AL, Biton M, Rogel N, Herbst RH, Shekhar K, Smillie C, et al. 2017. A single-cell survey of the small intestinal epithelium. *Nature*, **551**(7680): 333−339.

Han XP, Zhou ZM, Fei LJ, Sun HY, Wang RY, Chen Y, et al. 2020. Construction of a human cell landscape at single-cell level. *Nature*, **581**(7808): 303−309.

Jenkins G, Tortora GJ. 2016. Anatomy and Physiology. 6th ed. Hoboken: John Wiley & Sons.

Joost S, Zeisel A, Jacob T, Sun XY, La Manno G, Lönnerberg P, et al. 2016. Single-cell transcriptomics reveals that differentiation and spatial signatures shape epidermal and hair follicle heterogeneity. *Cell Systems*, **3**(3): 221−237.e9.

Kanehisa M, Furumichi M, Sato Y, Ishiguro-Watanabe M, Tanabe M. 2021. KEGG: integrating viruses and cellular organisms. *Nucleic Acids Research*, **49**(D1): D545−D551.

Khan SF, Damerell V, Omar R, Du Toit M, Khan M, Maranyane HM, et al. 2020. The roles and regulation of TBX3 in development and disease. *Gene*, **726**: 144223.

Kim SH, Turnbull J, Guimond S. 2011. Extracellular matrix and cell signalling: the dynamic cooperation of integrin, proteoglycan and growth factor receptor. *Journal of Endocrinology*, **209**(2): 139−151.

Lei Y, Zhang K, Guo MM, Li GW, Li C, Li BB, et al. 2018. Exploring the spatial-temporal microbiota of compound stomachs in a pre-weaned goat model. *Frontiers in Microbiology*, **9**: 1846.

Ma ASP, Ozers LJ. 1996. Annexins I and II show differences in subcellular localization and differentiation-related changes in human epidermal keratinocytes. *Archives of Dermatological Research*, **288**(10): 596−603.

Martini F. 2006. Anatomy and Physiology'2007 Ed. Rex Bookstore, Inc.

Masunaga T, Shimizu H, Ishiko A, Fujiwara T, Hashimoto T, Nishikawa T. 1995. Desmoyokin/AHNAK protein localizes to the non-desmosomal keratinocyte cell surface of human epidermis. *Journal of Investigative Dermatology*, **104**(6): 941−945.

Mehic D, Bakiri L, Ghannadan M, Wagner EF, Tschachler E. 2005. Fos and jun proteins are specifically expressed during differentiation of human keratinocytes. *Journal of Investigative Dermatology*, **124**(1): 212−220.

Mizrahi I, Jami E. 2018. Review: The compositional variation of the rumen microbiome and its effect on host performance and methane emission. *Animal*, **12**(s2): s220−s232.

Naeem A, Drackley JK, Stamey J, Loor JJ. 2012. Role of metabolic and cellular proliferation genes in ruminal development in response to enhanced plane of nutrition in neonatal Holstein calves. *Journal of Dairy Science*, **95**(4): 1807−1820.

Ogawa E, Owada Y, Ikawa S, Adachi Y, Egawa T, Nemoto K, et al. 2011. Epidermal FABP (FABP5) regulates keratinocyte differentiation by 13(S)-HODE-mediated activation of the NF-κB signaling pathway. *Journal of Investigative Dermatology*, **131**(3): 604−612.

Oshima T, Gedda K, Koseki J, Chen X, Husmark J, Watari J, et al. 2011. Establishment of esophageal-like non-keratinized stratified epithelium using normal human bronchial epithelial cells. *American Journal of Physiology-Cell Physiology*, **300**(6): C1422−C1429.

Pan XY, Wang Y, Li ZJ, Chen XQ, Heller R, Wang NN, et al. 2020. Tracing the origin of a new organ by inferring the genetic basis of rumen evolution. *bioRxiv*,doi: 10.1101/2020.02.19.955872.

Pazoki A, Ghorbani GR, Kargar S, Sadeghi-Sefidmazgi A, Drackley JK, Ghaffari MH. 2017. Growth performance, nutrient digestibility, ruminal fermentation, and rumen development of calves during transition from liquid to solid feed: Effects of physical form of starter feed and forage provision. *Animal Feed Science and Technology*, **234**: 173−185.

Peres J, Mowla S, Prince S. 2015. The T-box transcription factor, TBX3, is a key substrate of AKT3 in melanomagenesis. *Oncotarget*, **6**(3): 1821−1833.

Perng YC, Lenschow DJ. 2018. *ISG15* in antiviral immunity and beyond. *Nature Reviews Microbiology*, **16**(7): 423−439.

Prenzler F, Fragasso A, Schmitt A, Munz B. 2016. Functional analysis of ZFP36 proteins in keratinocytes. *European Journal of Cell Biology*, **95**(8): 277−284.

Rémond D, Ortigues I, Jouany JP. 1995. Energy substrates for the rumen epithelium. *Proceedings of the Nutrition Society*, **54**(1): 95−105.

Russell JB, Rychlik JL. 2001. Factors that alter rumen microbial ecology. *Science*, **292**(5519): 1119−1122.

Schoenberger SP. 2012. CD69 guides $CD4^+$ T cells to the seat of memory. *Proceedings of the National Academy of Sciences of the United States of America*, **109**(22): 8358−8359.

Steele MA, AlZahal O, Hook SE, Croom J, Mcbride BW. 2009. Ruminal acidosis and the rapid onset of ruminal parakeratosis in a mature dairy cow: a case report. *Acta Veterinaria Scandinavica*, **51**(1): 39.

Steven AC, Steinert PM. 1994. Protein composition of cornified cell envelopes of epidermal keratinocytes. *Journal of Cell Science*, **107**(2): 693−700.

Steven D, Marshall A, Phillipson A. 1970. Organization of the rumen epithelium. Physiology of digestion and metabolism in the ruminant. *In*: Proceedings of the third international symposium. Cambridge, England, Newcastle-upon-Tyne: Oriel Press.

Storesund T, Schenck K, Osmundsen H, Røed A, Helgeland K, Kolltveit KM. 2009. Signal transduction and gene transcription induced by TFF3 in oral keratinocytes. *European Journal of Oral Sciences*, **117**(5): 511−517.

Underwood WJ, Blauwiekel R, Delano ML, Gillesby R, Mischler SA, Schoell A. 2015. Biology and diseases of ruminants (sheep, goats, and cattle). *In*: Fox JG, Anderson LC, Otto GM, Pritchett-Corning KR, Whary MT. Laboratory Animal Medicine. Amsterdam: Elsevier, 623–694.

Vijayan A, Guha D, Ameer F, Kaziri I, Mooney CC, Bennett L, et al. 2013. IGFBP-5 enhances epithelial cell adhesion and protects epithelial cells from TGFβ1-induced mesenchymal invasion. *The International Journal of Biochemistry & Cell Biology*, **45**(12): 2774−2785.

Wagner T, Beer L, Gschwandtner M, Eckhart L, Kalinina P, Laggner M, et al. 2019. The differentiation-associated keratinocyte protein cornifelin contributes to cell-cell adhesion of epidermal and mucosal keratinocytes. *Journal of Investigative Dermatology*, **139**(11): 2292−2301.9.

Wang SX, Drummond ML, Guerrero-Juarez CF, Tarapore E, MacLean AL, Stabell AR, et al. 2020. Single cell transcriptomics of human epidermis identifies basal stem cell transition states. *Nature Communications*, **11**(1): 4239.

Wang YO, Brieher WM. 2020. CD2AP links actin to PI3 kinase activity to extend epithelial cell height and constrain cell area. *Journal of Cell Biology*, **219**(1): e201812087.

Wani SA, Sahu AR, Khan RIN, Pandey A, Saxena S, Hosamani N, et al. 2019. Contrasting gene expression profiles of monocytes and lymphocytes from peste-des-petits-ruminants virus infected goats. *Frontiers in Immunology*, **10**: 1463.

Webster JD, Vucic D. 2020. The balance of TNF mediated pathways regulates inflammatory cell death signaling in healthy and diseased tissues. *Frontiers in Cell and Developmental Biology*, **8**: 365.

Wise GH, Anderson GW. 1939. Factors affecting the passage of liquids into the rumen of the dairy calf. I. Method of administering liquids: drinking from open pail versus sucking through a rubber nipple. *Journal of Dairy Science*, **22**(9): 697−705.

Xia C, Braunstein Z, Toomey AC, Zhong JX, Rao XQ. 2018. S100 proteins As an important regulator of macrophage inflammation. *Frontiers in Immunology*, **8**: 1908.

Xu QB, Qiao QQ, Gao Y, Hou JX, Hu MY, Du YF, et al. 2021. Gut microbiota and their role in health and metabolic disease of dairy cow. *Frontiers in Nutrition*, **8**: 701511.

Yang Z, Bowles NE, Scherer SE, Taylor MD, Kearney DL, Ge SP, et al. 2006. Desmosomal dysfunction due to mutations in desmoplakin causes arrhythmogenic right ventricular dysplasia/cardiomyopathy. *Circulation Research*, **99**(6): 646−655.